HHS Public Access

Author manuscript

Cell Rep. Author manuscript; available in PMC 2016 April 20.

Published in final edited form as:

Cell Rep. 2016 April 19; 15(3): 563–573. doi:10.1016/j.celrep.2016.03.055.

Differential Dopamine Regulation of Ca^{2+} Signaling and Its Timing Dependence in the Nucleus Accumbens

Immani Swapna, **Brian Bondy**, and **Hitoshi Morikawa**

Department of Neuroscience and Waggoner Center for Alcohol and Addiction Research, University of Texas at Austin, Austin, Texas 78712

SUMMARY

Dopamine action in the nucleus accumbens (NAc) is thought to drive appetitive behavior and Pavlovian reward learning. However, it remains controversial how dopamine achieves these behavioral effects by regulating medium spiny projection neurons (MSNs) of the NAc, especially on a behaviorally relevant timescale. Metabotropic glutamate receptor (mGluR)-induced Ca^{2+} signaling dependent on the Ca^{2+}- releasing messenger inositol 1,4,5-triphosphate (IP_3) plays a critical role in controlling neuronal excitability and synaptic plasticity. Here, we show that transient dopamine application facilitates mGluR/IP_3-induced Ca^{2+} signals within a time window of ~2–10 s in a subpopulation of MSNs in the NAc core. Dopamine facilitation of IP_3-induced Ca^{2+} signaling is mediated by D1 dopamine receptors. In dopamine-insensitive MSNs, activation of A2A adenosine receptors causes enhancement of IP_3-evoked Ca^{2+} signals, which is reversed by D2 dopamine receptor activation. These results show that dopamine differentially regulates Ca^{2+} signaling on the order of seconds in two distinct MSN subpopulations.

INTRODUCTION

The nucleus accumbens (NAc), which constitutes major part of the ventral striatum, plays a critical role in driving appetitive behavior, Pavlovian reward learning, and the development of addiction (Day and Carelli, 2007; Fields et al., 2007; Ikemoto and Bonci, 2014). It receives massive dopaminergic projections from the ventral tegmental area (VTA), forming the mesolimbic dopaminergic system. Dopamine (DA) neurons in the VTA and the adjacent substantia nigra display transient increases in firing frequency, or bursts, in response to unexpected primary rewards or to reward-predicting environmental cues after repeated cue-reward conditioning (Schultz, 1998), eliciting phasic DA transients lasting several seconds in the NAc and other target areas (Day et al., 2007; Phillips et al., 2003). Ample evidence implicates these DA transients in motivating goal-directed behaviors aimed at rewards or reward-predicting cues and in the learning of cues and behaviors leading to rewards. These

*Correspondence: morikawa@utexas.edu, 1-512-232-9299.

AUTHOR CONTRIBUTIONS

I.S. and B.B. conducted the experiments and analyzed the data. I.S. and H.M. designed the experiments and wrote the paper.

behavioral effects are thought to arise from short-term and long-term actions of DA on intrinsic excitability and synaptic transmission in medium spiny neurons (MSNs), projection neurons of the NAc/striatum (Gerfen and Surmeier, 2011; Luscher and Malenka, 2011).

Intracellular Ca^{2+} signaling, triggered by either action potentials (APs) or synaptic inputs, dynamically controls neuronal activity and plasticity via its actions on plasma membrane ion channels, cytosolic enzymes, and other Ca^{2+}-sensitive proteins (Augustine et al., 2003; Berridge, 1998; Fakler and Adelman, 2008). Although Ca^{2+} influx through voltage-gated Ca^{2+} channels or Ca^{2+}-permeable ionotropic neurotransmitter receptors (e.g., NMDA-type glutamate receptors) provides the major source of Ca^{2+}, release of Ca^{2+} from intracellular stores also make significant contributions. In particular, it has been shown that AP-evoked Ca^{2+} signals can be amplified by preceding activation of group I metabotropic glutamate receptors (mGluRs) coupled to the generation of inositol-1,4,5-triphosphate (IP_3) in DA neurons, hippocampal pyramidal neurons, and cerebellar Purkinje neurons (Cui et al., 2007; Nakamura et al., 2000; Wang et al., 2000). Here, IP_3 increases the sensitivity of IP_3 receptors (IP_3Rs) to Ca^{2+}-dependent activation (Doi et al., 2005; Taylor and Laude, 2002), thereby enhancing Ca^{2+}-induced Ca^{2+} release (CICR) from intracellular stores triggered by AP-induced Ca^{2+} influx. Furthermore, strong activation of mGluRs and other IP_3-coupled neurotransmitter receptors produces large Ca^{2+} increases by itself without AP-evoked Ca^{2+} influx in diverse CNS neurons, frequently causing hyperpolarizations mediated by Ca^{2+}-sensitive K^+ conductances (Canepari and Ogden, 2006; El-Hassar et al., 2011; Fiorillo and Williams, 2000; Gulledge and Stuart, 2005; Hagenston et al., 2008; Morikawa et al., 2003; Power and Sah, 2008). These forms of IP_3-dependent Ca^{2+} signaling have been recently reported in MSNs of the dorsal striatum (Clements et al., 2013; Partridge et al., 2014; Plotkin et al., 2013). However, it remains largely unknown how DA regulates IP_3-induced Ca^{2+} signals in MSNs or in any other CNS neurons.

The expression of D1 and D2 DA receptors, two predominant DA receptor subtypes, is mostly segregated into distinct subpopulations of MSNs in the NAc (Bertran-Gonzalez et al., 2008; Bertran-Gonzalez et al., 2010; Frederick et al., 2015; Smith et al., 2013), as has been shown in the dorsal striatum (Gerfen et al., 1990; Gerfen and Surmeier, 2011; Surmeier et al., 1996) [but also see (Perreault et al., 2014) for expression of D1–D2 receptor heteromers in certain MSNs]. In this study, using ex vivo slices from mice, we investigated how DA differentially regulates mGluR/IP_3-dependent Ca^{2+} signaling via D1 and D2 receptors in the NAc core, the subregion predominantly involved in the formation and expression of cue-reward memory (Saddoris et al., 2013; Sesack and Grace, 2010).

RESULTS

Phasic DA Enhances IP_3-Induced Ca^{2+} Signals in a Timing-Dependent Manner in a Subset of MSNs

Whole-cell voltage clamp recordings of MSNs were made in the NAc core. MSNs were held at −57 mV, which is close to membrane potentials during the up-state where MSNs frequently fire trains of APs (Stern et al., 1998; Wickens and Wilson, 1998; Wilson and Kawaguchi, 1996). To examine DA action on IP_3-dependent Ca^{2+} signaling, IP_3 was directly applied into the cytosol using UV photolysis of caged IP_3. Our previous study in striatal

MSNs has shown that photolytic IP_3 application produces a transient rise in $[Ca^{2+}]_i$, together with a transient outward current via Ca^{2+}-sensitive K^+ conductances (termed I_{IP3}), in a concentration-dependent manner when the UV flash intensity is varied (Clements et al., 2013). In the current experiments, UV flash intensity was adjusted to evoke relatively small outward currents (15–60 pA using $<EC_{50}$ IP_3 concentration; see Experimental Procedures for details). I_{IP3} thus evoked was virtually eliminated by apamin (100 nM, n = 5 cells; Figure 1A), a selective blocker of small-conductance Ca^{2+}-activated K^+ (SK) channels, which are solely gated by Ca^{2+} (Fakler and Adelman, 2008). To mimic phasic DA transients observed in the NAc in behaving animals (Day et al., 2007; Phillips et al., 2003), DA (20 μM) was pressure ejected for 2.5 s from a pipette placed ~100 μm from the recorded MSN. When DA application was made prior to photolytic IP_3 application (5 s interval between the onset of 2.5 s DA application and UV flash), DA produced measurable (≥18%) increases in I_{IP3} in 30 out of 61 recorded MSNs (Figures 1B, 1C, and S1). DA application had no measurable effect on the holding current in these cells (data not shown). We further directly monitored intracellular Ca^{2+} ($[Ca^{2+}]_i$) at the soma using the low-affinity Ca^{2+} indicator Fluo-4FF (100 μM) loaded into the cytosol via the whole-cell pipette (>20 min). Phasic DA application increased IP_3-evoked Ca^{2+} transients (with 5 s interval) in 6 out of 11 MSNs tested (Figures 1D and 1E).

We next varied the interval between phasic DA onset and photolytic IP_3 application in DA responsive MSNs (n = 6 cells; Figures 1F and 1G). DA caused I_{IP3} facilitation with 2–5 s interval, an effect that decayed when the interval was prolonged to 10–20 s. No effect was observed when phasic DA onset was simultaneous with photolytic IP_3 application. Therefore, phasic DA facilitates IP_3-evoked Ca^{2+} signals with a time window of ~2–10 s in MSNs of the NAc core.

Phasic DA Prolongs IP_3-Induced Pauses in MSN Firing

It has been shown in the dorsal striatum that mGluR/IP_3-induced Ca^{2+} signals drive pauses in MSN firing resulting from SK channel-dependent hyperpolarization (Clements et al., 2013). To test the effect of phasic DA on IP_3-induced firing pauses, current clamp recordings of MSNs were made in the NAc core. AP firing was evoked by 4 s depolarizing current injections (~200–400 pA; adjusted to produce ~5–10 Hz firing), during which photolytic IP_3 application was made 2 s after the onset of current injection (Figure 2; UV flash intensity was adjusted in voltage clamp). Phasic DA application (2.5 s; onset 5 s prior to UV flash, i.e., 3 s prior to the onset of current injection) failed to affect MSN firing preceding IP_3 application in all 7 cells tested. However, phasic DA prolonged IP_3-evoked pauses in 3 cells that displayed DA-induced I_{IP3} facilitation in voltage clamp, while DA had no effect in the remaining 4 cells (Figures 2 and S2).

mGluR Activation Facilitates Ca^{2+} Signals Evoked by Trains of APs in NAc MSNs

mGluR/IP_3-dependent amplification of AP-evoked Ca^{2+} signals has been implicated in driving synaptic plasticity in CNS neurons (Harnett et al., 2009; Wang et al., 2000). To assess AP-evoked Ca^{2+} signals in MSNs, 2 ms depolarizing pulses of 30 mV were applied to evoke unclamped APs and the resulting tail outward currents were recorded, similarly to our previous study in the dorsal striatum (Clements et al., 2013). We first confirmed that these

tail currents, evoked by a single AP ($I_{AP\text{-}single}$) or a 200 ms AP train (5 APs at 20 Hz; $I_{AP\text{-}train}$), were completely eliminated by TTX (1 μM) in the NAc (n = 4 cells; Figure S3A). Furthermore, $I_{AP\text{-}single}$ and $I_{AP\text{-}train}$ were suppressed by apamin (100 nM, n = 4 cells; Figure S3B). The apamin-insensitive component of $I_{AP\text{-}single}$ and $I_{AP\text{-}train}$ mostly decayed within 50 ms and 150 ms, respectively, except for a small component of $I_{AP\text{-}train}$ that slowly decayed over ~5–10 s.

To investigate mGluR/IP_3-dependent regulation AP-evoked Ca^{2+} signals, we tested the effect of DHPG, a group I mGluR (mGluR1/5) agonist, on $I_{AP\text{-}single}$ and $I_{AP\text{-}train}$. Bath application of DHPG (5 μM; 3–5 min) added a late component to $I_{AP\text{-}single}$ in 3 out of 7 cells tested, while $I_{AP\text{-}train}$ was consistently augmented and prolonged by DHPG in a reversible manner in all of these cells (Figures 3A and S4). In order to quantify the DHPG effect on $I_{AP\text{-}single}$ and $I_{AP\text{-}train}$, we calculated the time integral of these currents after removing the initial 50 ms or 150 ms window, respectively (termed Q-K(Ca); current level at ~600–800 ms after the AP train offset was taken as baseline for $I_{AP\text{-}train}$) (Figure 3A). It should be noted that apamin completely eliminated the DHPG effect on $I_{AP\text{-}train}$ (n = 6 cells; Figure S3C), supporting the use of the SK-dependent component of $I_{AP\text{-}train}$ as a measure of mGluR-induced Ca^{2+} signal regulation. In the following experiments, we focused on Ca^{2+} signals evoked by AP trains (5 APs at 20 Hz) in light of the consistency and robustness of DHPG-induced enhancement.

When $[Ca^{2+}]_i$ was monitored at the soma with Fluo-4FF (100 μM), DHPG (5 μM) produced large increase and prolongation of AP train-evoked Ca^{2+} signals (n = 5 cells; Figure 3B). Increasing the concentration of Fluo-4FF to 500 μM significantly attenuated the DHPG effect on AP train-evoked Ca^{2+} transients (n = 4 cells; Figure S5), reflecting an increase in the Ca^{2+} buffering capacity. Altogether, these results show that mGluR activation amplifies Ca^{2+} signals triggered by AP trains in MSNs of the NAc core.

To examine whether facilitation of AP train-evoked Ca^{2+} signals is caused via CICR, we tested cyclopiazonic acid (CPA), which depletes intracellular Ca^{2+} stores (Seidler et al., 1989). Bath application of CPA (20 μM; >10 min), which inhibited $I_{AP\text{-}train}$ by itself, completely eliminated DHPG-induced facilitation (Figures 3C and 3E). Furthermore, intracellular application of heparin (0.1–0.25 mg/ml; >20 min dialysis via the whole-cell pipette), an IP_3R antagonist (Ghosh et al., 1988), also largely suppressed the DHPG effect on $I_{AP\text{-}train}$ (Figures 3D and 3E). To further demonstrate the role of IP_3, we performed UV photolysis of caged IP_3 at subthreshold intensity, which produced no measurable rise in $[Ca^{2+}]_i$ by itself. However, this subthreshold IP_3 caused significant facilitation of AP train-evoked Ca^{2+} transients when applied 50 ms prior to the AP train (Figures 3F and 3G), in a manner analogous to DHPG perfusion. Therefore, IP_3-dependent CICR underlies mGluR facilitation of AP train-evoked Ca^{2+} signals.

Phasic DA Amplifies IP_3 Facilitation of AP Train-Evoked Ca^{2+} Signals in a Subset of MSNs

We next investigated how phasic DA affects IP_3-dependent regulation AP train-evoked Ca^{2+} signals. Transient DA application (2.5 s, onset 5 s prior to the AP train) failed to exert measurable effect on AP train-evoked Ca^{2+} transients in 9 cells tested (loaded with 100 μM Fluo-4FF; Figures 4A and 4B). However, DA caused >20% increases in AP train-evoked

Ca^{2+} transients when facilitated by subthreshold IP_3 in 5 out of these 9 cells (Figures 4A–4C). Hence, phasic DA can amplify the facilitatory effect of IP_3 on AP train-evoked Ca^{2+} signals in a subset of MSNs in the NAc core.

D1 DA Receptors Mediate Enhancement of IP_3-Induced Ca^{2+} Signals

To address the involvement of DA receptor subtypes in Ca^{2+} signal regulation, we examined the effects of the D1 agonist SKF81297 and the D2 agonist quinpirole on I_{IP3} (UV flash intensity set as in Figures 1 and 2). Bath application of SKF81297 (1 μM) increased I_{IP3} by >20% in 15 out of 27 cells tested (Figures 5A and 5C). This SKF8129-induced I_{IP3} facilitation was reversed by the D1 antagonist SCH23390 (1 μM; n = 7). In contrast, the D2 agonist quinpirole (1 μM) failed to affect I_{IP3} in all MSNs tested (n = 9; Figures 5B and 5C). Furthermore, phasic DA-induced facilitation of I_{IP3} was completely blocked by SCH23390 (n = 5; Figures 5D–5F), demonstrating the role of D1 receptors in phasic DA action.

D2 DA Receptors Mediate Reversal of A2A Adenosine Receptor-Induced Ca^{2+} Signal Facilitation in D1-Insensitive MSNs

D1 and D2 receptors are coupled to G_s- and G_i-subtype G proteins, which stimulate and inhibit the adenylyl cyclase-cAMP-PKA (protein kinase A) pathway, respectively. Adensoine A2A receptors, which are coupled to G_s like D1 receptors, are selectively expressed in D2 receptor-positive MSNs, where they frequently exert effects opposing those mediated by G_i-coupled D2 receptors (Higley and Sabatini, 2010; Schiffmann et al., 2007; Shen et al., 2008). Thus we examined the effect of the A2A receptor agonist CGS21680 (1 μM) on I_{IP3}. In 12 cells tested for both SKF81297 and CGS21680 (SKF81297 tested first in 8 cells, CGS21680 tested first in 4 cells), we found that CGS21680 augmented I_{IP3} in 6 cells that displayed no response to SKF81297 (Figures 6A and 6B), while CGS21680 had no effect in 6 cells in which SKF81297 facilitated I_{IP3} (Figures 6C and 6D). CGS21680 increased I_{IP3} in 5 out of 11 cells where CGS21680 was tested without prior SKF81297 application. CGS21680-induced I_{IP3} facilitation was reversed by the A2A receptor antagonist SCH58261 (1 μM, n = 4; Figure 6A). Furthermore, in 12 MSNs tested for phasic DA effect on I_{IP3}, CGS21680 increased I_{IP3} in 7 cells in which phasic DA application had no effect (Figure 6E), whereas CGS21680 was ineffective in 5 cells that responded to phasic DA (Figure 6F). These results demonstrate that D1 DA receptors and A2A adenosine receptors positively regulate IP_3-dependent Ca^{2+} signaling in distinct, non-overlapping subpopulations of MSNs.

Finally, the D2 agonist quinpirole, which had no effect on I_{IP3} by itself (Figures 5B and 5C), was capable of reversing CGS21680-induced I_{IP3} facilitation, at least partially, in all 5 cells tested (Figures 7A–7C), while quinpirole failed to reverse the SKF81297 effect (5 cells; Figures 7D–7F). Similarly, phasic DA application caused reversal of CGS21680-induced I_{IP3} facilitation (Figures 7G–7I; tested in 4 cells out of the 7 cells shown in Figure 7F where phasic DA failed to affect I_{IP3} by itself). These results are consistent with the selective expression of D2 receptors in A2A receptor-positive MSNs, where activation of D2 receptors counteracts A2A receptor-mediated enhancement of IP_3-dependent Ca^{2+} signaling.

DISCUSSION

Previous studies in the dorsal striatum have shown that D1 DA receptors and A2A adenosine receptors mediate facilitation of NMDA receptor-induced Ca^{2+} signals in distinct subpopulations of MSNs in the dorsal striatum, with A2A receptor-mediated facilitation being reversed by D2 receptor activation (Higley and Sabatini, 2010; Plotkin et al., 2011). The present study demonstrates that mGluR/IP_3-induced Ca^{2+} signaling undergoes similar regulation by these receptors (D1 vs. A2A/D2) in two distinct MSN subpopulations in the NAc. Thus DA controls two types of Ca^{2+} signals that play critical roles in regulating MSN excitability and plasticity. Intriguingly, DA puff application (2.5 s), mimicking phasic DA transients observed in behaving animals (Day et al., 2007; Phillips et al., 2003), triggered D1 receptor-mediated facilitation of IP_3-evoked Ca^{2+} signals when its onset preceded IP_3 application by ~2–10 s. This type of timing dependence of DA action in the order of seconds might be related to the timing dependence of reward action displayed during reward-based appetitive behavior and conditioning (Day and Carelli, 2007; Fields et al., 2007; Schultz, 1998).

Differential Regulation of IP_3-Evoked Ca^{2+} Signals in Two Subpopulations of MSNs

Phasic DA application enhanced IP_3-evoked Ca^{2+} signals in ~50% of MSNs (30 out of 61 cells) in the NAc core. This DA effect is mediated by D1 receptors, as it was blocked by a D1 antagonist and reproduced by a D1 agonist. We further found that, in the remaining subpopulation of MSNs displaying no D1 response, A2A adenosine receptors drive facilitation of IP_3-evoked Ca^{2+} signals, which can be reversed by D2 receptor activation, attained with either phasic DA or a D2 agonist. In contrast to many recent brain slice recording studies using transgenic mice in which MSNs expressing D1 or D2 receptors are selectively labeled with markers (e.g., green fluorescent proteins) (Higley and Sabatini, 2010; Lim et al., 2012; Pascoli et al., 2014; Plotkin et al., 2011), recordings were done in NAc slices from wild-type mice in the present study. Thus the experimenter was "blind" in terms of the MSN subtypes (D1 receptor-expressing vs. D2 receptor-expressing) during recording and still was able to detect two distinct, nonoverlapping subsets of MSNs: one showing D1-mediated response and the other displaying counteracting effects of A2A/D2 receptors. Coexpression of D1 and D2 receptors has been shown in a small fraction of MSNs (2–6 %) in the NAc core in transgenic mice (Bertran-Gonzalez et al., 2008; Kupchik et al., 2015). We failed to observe MSNs displaying both D1 and D2 responses, i.e., D1-mediated Ca^{2+} signal facilitation reversed by D2 activation, or MSNs responsive to both D1 and A2A activation, with latter being reversed by D2 activation. It should also be noted that phasic DA application caused no Ca^{2+} rises by itself in the present study, in contrast to the evidence for the existence of D1–D2 heteromers coupled to IP_3-induced Ca^{2+} signaling in certain MSNs in rats (Hasbi et al., 2010). Thus, DA regulation of IP_3-induced Ca^{2+} signaling may display regional difference (NAc core vs. NAc shell vs. dorsal striatum) and/or species difference based on the degree of D1–D2 coexpression/heterodimerization (Bertran-Gonzalez et al., 2010; Perreault et al., 2014).

Mechanistically, PKA phosphorylation of IP_3Rs is known to increase their IP_3 sensitivity (Tang et al., 2003; Wagner et al., 2008). Alternatively, recent studies indicate that cAMP can

directly increase IP_3R sensitivity independent of PKA phosphorylation (Taylor et al., 2014; Tovey et al., 2010). These mechanisms most likely underlie the differential regulation via D1 receptors (G_s-coupled) vs. A2A receptors (G_s-coupled)/D2 receptors (G_i-coupled) in two MSN subpopulations. The ineffectiveness of D2 activation in regulating basal IP_3-evoked Ca^{2+} signals (i.e., without A2A-induced facilitation) suggests low basal cAMP levels/PKA activity in MSNs, which may be reflecting low adenosine tone in ex vivo slices [(Plotkin et al., 2011); but also see (Higley and Sabatini, 2010)].

Regulation of AP-Evoked Ca^{2+} Signals: Interaction between D1 DA receptors and mGluRs Coupled to IP_3 Generation

Our data demonstrate that mGluR activation facilitates AP train-evoked Ca^{2+} signals via IP_3-dependent CICR in MSNs of the NAc core, as has been reported in DA neurons, hippocampal pyramidal neurons, and cerebellar Purkinje neurons (Cui et al., 2007; Nakamura et al., 2000; Wang et al., 2000), as well as in MSNs of the dorsal striatum (Plotkin et al., 2013). mGluR action on single AP-evoked Ca^{2+} signals was inconsistent among MSNs, in contrast to the robust mGluR-induced facilitation of single AP-evoked Ca^{2+} signals observed in DA neurons of the substantia nigra (Cui et al., 2007). Thus, in MSNs, large Ca^{2+} influx associated with multiple APs is necessary to reliably trigger Ca^{2+}-dependent activation of IP_3Rs driving regenerative CICR, even when their Ca^{2+} sensitivity is increased by IP_3 generated via mGluR activation.

As expected from the D1-dependent regulation of IP_3 signaling, phasic DA is capable of promoting IP_3 facilitation of AP train-evoked Ca^{2+} signals in a subset of MSNs, while having no effect on basal AP train-evoked Ca^{2+} signals. Ryanodine receptors (RyRs), another type of Ca^{2+}-activated receptors on intracellular Ca^{2+} stores, have been shown to selectively mediate the CICR-dependent component of basal AP train-evoked Ca^{2+} transients in MSNs of the dorsal striatum (Clements et al., 2013). Our data suggest that RyR-mediated CICR cannot be directly regulated by D1 activation; however RyRs may well act to boost IP_3R-dependent CICR (Plotkin et al., 2013), particularly when the latter is facilitated by D1 activation.

Previous studies have shown that D2 activation, either by focal DA puff application or bath perfusion of the D2 agonist quinpirole, suppresses AP-evoked Ca^{2+} transients in dendritic spines of D2 receptor-expressing MSNs in the dorsal striatum (Day et al., 2008; Higley and Sabatini, 2010), while another study has reported that optogenetic stimulation of dopaminergic fibers has no effect on AP-evoked Ca^{2+} transients in dendritic spines of D1 receptor-expressing MSNs in the NAc core (Yagishita et al., 2014). Although out of the scope of the current study, it would be interesting to fully determine DA actions on AP-evoked Ca^{2+} transients, both basal and IP_3-facilitated, in different subcellular locations of MSNs, as has been demonstrated for DA-induced activation of PKA (soma/proximal dendrites vs. distal dendrites) in the Yagishita et al. study.

Timing Dependence of DA Effect on IP_3 Signaling: Potential Relevance to Phasic DA Actions in Behaving Animals

In behaving animals, presentation of primary rewards or reward-predicting sensory stimuli evokes transient DA rises in the NAc core lasting ~1–10 s (Day and Carelli, 2007; Day et al., 2007; Phillips et al., 2003). Although the critical roles of these phasic DA signals in driving reward-based learning and motivated behavior is widely agreed upon, the precise mechanisms underlying DA actions in the NAc/striatum remain to be a matter of debate (Fields et al., 2007; Surmeier et al., 2014; Tritsch and Sabatini, 2012). How exactly do phasic DA signals affect MSNs? The answer to this question has been elusive, as DA exerts no clear effects on MSNs in the order of seconds. For example, a recent study reported a form of phasic DA-timing-dependent synaptic plasticity, where phasic DA paired with synaptic activity within a time window of ~1 s, while having no immediate effects on MSN activity or synaptic transmission by itself, leads to persistent synaptic potentiation after the pairing (Wieland et al., 2015). In line with the lack of acute DA effects on MSNs, another recent study has exogenously expressed G protein-coupled inwardly rectifying K^+ channels (GIRKs) as a "sensor" to detect phasic DA-evoked activation of D2 receptors with high temporal resolution (i.e., in the order of seconds) in MSNs (Marcott et al., 2014). Our data demonstrate that activation of D1 receptors with local DA application (2.5 s) leads to transient facilitation of IP_3-evoked Ca^{2+} signaling within 2 s from the onset of DA application, peaking at 5 s, and lasting for ~10 s to 20 s at most. Intriguingly, phasic DA activation of D1 receptors, attained with photolytic DA application (0.1–1 s), has been shown to produce PKA activation within seconds, peaking at ~20–30 s, and lasting for ~1–3 min in striatal MSNs (Castro et al., 2013). Similarly, phasic DA release via optogenetic stimulation of DA fibers (0.3 s), when paired with AP train-evoked Ca^{2+}rises necessary to activate Ca^{2+}-sensitive adenylyl cyclase, causes D1-dependent PKA activation lasting ~1 min in dendritic spines of MSNs in the NAc core (Yagishita et al., 2014). Based on the difference in the onset/offset kinetics of DA action, direct cAMP regulation of IP_3Rs (Taylor et al., 2014; Tovey et al., 2010), not PKA phosphorylation of IP_3Rs (Tang et al., 2003; Wagner et al., 2008), may underlie the relatively rapid and short-lasting DA effect on IP_3-induced Ca^{2+} signaling demonstrated in the present study.

Firing pauses in a subpopulation of NAc neurons have been linked to reward-directed behavior (Krause et al., 2010; Taha and Fields, 2006). Furthermore, mGluR/IP_3-dependent amplification of AP-evoked Ca^{2+} signals is known to mediate the induction of glutamatergic synaptic plasticity in DA neurons and cerebellar Purkinje neurons (Harnett et al., 2009; Wang et al., 2000). We propose that DA-timing-dependent regulation of IP_3 signaling (i.e., IP_3-evoked pauses in firing and IP_3-induced facilitation of AP train Ca^{2+} transients) might play important roles during reward-based learning and behavior.

EXPERIMENTAL PROCEDURES

Animals

Male C57BL/6J mice (4–5 weeks old) were obtained from Jackson Laboratory and were housed under a 12 h light/dark cycle. Food and water were available *ad libitum*. All animal

procedures were approved by the University of Texas Institutional Animal Care and Use Committee.

Electrophysiology

Mice were sacrificed by cervical dislocation under isoflurane anesthesia and the brain was quickly dissected out. Coronal or sagittal slices (200–250 μm) containing the NAc were cut in an ice-cold solution containing (in mM): 205 sucrose, 2.5 KCl, 1.25 NaH_2PO_4, 7.5 $MgCl_2$, 0.5 $CaCl_2$, 10 glucose, and 25 $NaHCO_3$, saturated with 95% O_2 and 5% CO_2 (~300 mOsm/kg) and incubated > 1 h at 35°C in physiological saline containing (in mM): 126 NaCl, 2.5 KCl, 1.2 NaH_2PO_4, 1.2 $MgCl_2$, 2.4 $CaCl_2$, 11 glucose, and 25 $NaHCO_3$, saturated with 95% O_2 and 5% CO_2 (pH 7.4, ~295 mOsm/ kg). MK-801 (10 μM) was added to the incubation chamber to prevent NMDA receptor-mediated toxicity. Recordings were made at 34–35°C in the same saline (without MK-801) perfused at ~2.5 ml/min. The majority of experiments were performed in the presence of DNQX (10 μM) and picrotoxin (100 μM) to block AMPA/$GABA_A$-mediated synaptic inputs.

Cells were visualized using an upright microscope (Olympus) with infrared/oblique illumination optics. Recordings were performed in the NAc core, which was located using anterior commissure as the landmark. Whole-cell recordings were made with borosilicate glass pipettes (2.0–2.6 MΩ) filled with internal solution containing (in mM): 115 K-gluconate, 20 KCl, 1.5 $MgCl_2$, 10 HEPES, 0.025 EGTA, 2 Mg-ATP, 0.2 Na_2-GTP, and 10 Na_2-phosphocreatine (pH 7.2, ~285 mOsm/kg), unless indicated otherwise. Series resistance was continuously monitored but left uncompensated during voltage-clamp recording experiments. Recordings were discarded if the series resistance increased beyond 18 MΩ. Bridge balance was adjusted periodically (~every 2–3 min) during current-clamp recording experiments. The membrane potential was corrected for a liquid junction potential of −7 mV. Axopatch 1D or Multiclamp 700B amplifier (Molecular Devices) and AxoGraph X software (AxoGraph Scientific) were used to record and collect data (filtered at 1–10 kHz and digitized at 2–20 kHz for voltage-clamp recordings, filtered at 10 kHz and digitized at 20 kHz for current-clamp recordings). MSNs, which comprise the vast majority (>90–95% in rodents) of neurons in the NAc/striatum, were identified by their electrophysiological properties, including hyperpolarized resting membrane potentials (~−80 to –95 mV), low input resistance at resting potential (~40–100 MΩ), prominent inward rectification, and slow depolarizing ramp preceding AP firing during threshold depolarizations, as in our previous studies (Beatty et al., 2012; Clements et al., 2013).

Ca^{2+} Imaging

Fluorescence imaging of $[Ca^{2+}]_i$ was done using low-affinity Ca^{2+} indicator Fluo-4FF (K_d = 9.7 μM). Fluo-4FF (100 or 500 μM; no EGTA in these experiments) was loaded into the cell via the whole-cell pipette (>20 min dialysis after break-in). Images were taken at ~7–15 Hz using the Olympus Disk Spinning Unit Imaging System. After raw fluorescent signals from selected regions of interest (ROIs) were background subtracted at each time point, Ca^{2+} transients were expressed as $\Delta F/F_0 = (F(t) - F_0)/F_0$, where F_0 was determined as an average of F(t) over a 1 s baseline period. Brief artifacts accompanying UV flashes are omitted from the fluorescence traces in flash photolysis experiments.

Flash Photolysis

Cells were dialyzed with caged IP_3 (50 μM) through the whole-cell pipette. A brief UV flash (~1 ms) was applied with a xenon arc lamp driven by a photolysis system (Cairn Research) to rapidly photolyze caged IP_3 (~3 ms) (Walker et al., 1989). The UV flash was focused through a 60× objective onto a 350 μm area surrounding the recorded cell. The Cairn system has the capacity to vary the intensity of UV flash, which was measured at the tip of the objective (expressed in μJ). The degree of photolysis of caged compounds is known to be proportional to the UV flash intensity (McCray et al., 1980), thus the concentration of IP_3 released into the cytosol can be expressed in μM·μJ. In the experiments testing suprathreshold IP_3 responses, UV flash intensity was adjusted to evoke I_{IP3} with amplitude ~50% of that evoked by the largest flash intensity in our setup (~200 μJ, i.e., ~10,000 μM·μJ IP_3; I_{IP3} shows no sign of saturation). This produced I_{IP3} in the range of 15–60 pA (with UV intensity in the range of ~25–50 μJ, i.e., ~1250–2500 μM·μJ IP_3) in the majority of recorded MSNs. Cells with I_{IP3} outside of this range were excluded from the analysis. It should be noted that IP_3 concentration up to 80,000 μM·μJ failed to evoke saturating IP_3 responses in MSNs of the dorsal striatum in our previous study (Clements et al., 2013).

DA Pressure Ejection

Patch pipettes (~2–3 μm tip diameter), filled with DA (20 μM) and ascorbate (1.3 mM) dissolved in physiological saline, were placed ~100 μm from recorded cells, and pressure of 15 p.s.i. was applied using a TooheySpritzer Pressure System IIe. The speed and spatial range of puff application can be seen in Movie S1, where both the puff pipette and the whole-cell recording pipette are loaded with Alexa Fluor 594 (50 μM). DA solutions were made fresh every 1 hr or after each recording.

Drugs

Apamin, iberiotoxin, cyclopiazonic acid, DHPG, DNQX, picrotoxin, quinpirole, SKF81297, SCH23390, CGS21680, and SCH58261 were obtained from Tocris Biosciences. TTX was obtained from Alomone Labs. Fluo-4FF and Alexa Fluor 594 were purchased from Life Technologies. Caged IP_3 was a generous gift from Dr. Kamran Khodakhah at Albert Einstein College of Medicine. All other chemicals were from Sigma-RBI.

Data Analysis

Data are expressed as mean ± SEM. Statistical significance was determined by Student's t test or ANOVA followed by Bonferroni post hoc test. The difference was considered significant at $p < 0.05$.

Supplementary Material

Refer to Web version on PubMed Central for supplementary material.

Acknowledgments

We thank Dr. Kamran Khodakhah for the generous gift of caged IP_3 made in his lab. We also thank Dr. Michael Clements for acquiring some preliminary data and Jeremiah Lee for providing NAc slices for certain experiments. This work was funded by NIH grants DA015687 and AA015521.

REFERENCES

Augustine GJ, Santamaria F, Tanaka K. Local calcium signaling in neurons. Neuron. 2003; 40:331–346. [PubMed: 14556712]

Beatty JA, Sullivan MA, Morikawa H, Wilson CJ. Complex autonomous firing patterns of striatal low-threshold spike interneurons. J Neurophysiol. 2012; 108:771–781. [PubMed: 22572945]

Berridge MJ. Neuronal calcium signaling. Neuron. 1998; 21:13–26. [PubMed: 9697848]

Bertran-Gonzalez J, Bosch C, Maroteaux M, Matamales M, Herve D, Valjent E, Girault JA. Opposing patterns of signaling activation in dopamine D1 and D2 receptor-expressing striatal neurons in response to cocaine and haloperidol. The Journal of neuroscience : the official journal of the Society for Neuroscience. 2008; 28:5671–5685. [PubMed: 18509028]

Bertran-Gonzalez J, Herve D, Girault JA, Valjent E. What is the Degree of Segregation between Striatonigral and Striatopallidal Projections? Frontiers in neuroanatomy. 2010; 4

Canepari M, Ogden D. Kinetic, pharmacological and activity-dependent separation of two Ca2+ signalling pathways mediated by type 1 metabotropic glutamate receptors in rat Purkinje neurones. J Physiol. 2006; 573:65–82. [PubMed: 16497716]

Castro LR, Brito M, Guiot E, Polito M, Korn CW, Herve D, Girault JA, Paupardin-Tritsch D, Vincent P. Striatal neurones have a specific ability to respond to phasic dopamine release. J Physiol. 2013; 591:3197–3214. [PubMed: 23551948]

Clements MA, Swapna I, Morikawa H. Inositol 1,4,5-triphosphate drives glutamatergic and cholinergic inhibition selectively in spiny projection neurons in the striatum. J Neurosci. 2013; 33:2697–2708. [PubMed: 23392696]

Cui G, Bernier BE, Harnett MT, Morikawa H. Differential regulation of action potential- and metabotropic glutamate receptor-induced Ca2+ signals by inositol 1,4,5-trisphosphate in dopaminergic neurons. J Neurosci. 2007; 27:4776–4785. [PubMed: 17460090]

Day JJ, Carelli RM. The nucleus accumbens and Pavlovian reward learning. The Neuroscientist : a review journal bringing neurobiology, neurology and psychiatry. 2007; 13:148–159.

Day JJ, Roitman MF, Wightman RM, Carelli RM. Associative learning mediates dynamic shifts in dopamine signaling in the nucleus accumbens. Nat Neurosci. 2007; 10:1020–1028. [PubMed: 17603481]

Day M, Wokosin D, Plotkin JL, Tian X, Surmeier DJ. Differential excitability and modulation of striatal medium spiny neuron dendrites. J Neurosci. 2008; 28:11603–11614. [PubMed: 18987196]

Doi T, Kuroda S, Michikawa T, Kawato M. Inositol 1,4,5-trisphosphatedependent Ca2+ threshold dynamics detect spike timing in cerebellar Purkinje cells. J Neurosci. 2005; 25:950–961. [PubMed: 15673676]

El-Hassar L, Hagenston AM, D'Angelo LB, Yeckel MF. Metabotropic glutamate receptors regulate hippocampal CA1 pyramidal neuron excitability via Ca(2)(+) wave-dependent activation of SK and TRPC channels. J Physiol. 2011; 589:3211–3229. [PubMed: 21576272]

Fakler B, Adelman JP. Control of K(Ca) channels by calcium nano/microdomains. Neuron. 2008; 59:873–881. [PubMed: 18817728]

Fields HL, Hjelmstad GO, Margolis EB, Nicola SM. Ventral tegmental area neurons in learned appetitive behavior and positive reinforcement. Annu Rev Neurosci. 2007; 30:289–316. [PubMed: 17376009]

Fiorillo CD, Williams JT. Cholinergic inhibition of ventral midbrain dopamine neurons. J Neurosci. 2000; 20:7855–7860. [PubMed: 11027251]

Frederick AL, Yano H, Trifilieff P, Vishwasrao HD, Biezonski D, Meszaros J, Urizar E, Sibley DR, Kellendonk C, Sonntag KC, et al. Evidence against dopamine D1/D2 receptor heteromers. Mol Psychiatry. 2015; 20:1373–1385. [PubMed: 25560761]

Gerfen CR, Engber TM, Mahan LC, Susel Z, Chase TN, Monsma FJ Jr, Sibley DR. D1 and D2 dopamine receptor-regulated gene expression of striatonigral and striatopallidal neurons. Science. 1990; 250:1429–1432. [PubMed: 2147780]

Gerfen CR, Surmeier DJ. Modulation of striatal projection systems by dopamine. Annual review of neuroscience. 2011; 34:441–466.

Ghosh TK, Eis PS, Mullaney JM, Ebert CL, Gill DL. Competitive, reversible, and potent antagonism of inositol 1,4,5-trisphosphate-activated calcium release by heparin. J Biol Chem. 1988; 263:11075–11079. [PubMed: 3136153]

Gulledge AT, Stuart GJ. Cholinergic inhibition of neocortical pyramidal neurons. J Neurosci. 2005; 25:10308–10320. [PubMed: 16267239]

Hagenston AM, Fitzpatrick JS, Yeckel MF. MGluR-mediated calcium waves that invade the soma regulate firing in layer V medial prefrontal cortical pyramidal neurons. Cereb Cortex. 2008; 18:407–423. [PubMed: 17573372]

Harnett MT, Bernier BE, Ahn KC, Morikawa H. Burst-timing-dependent plasticity of NMDA receptor-mediated transmission in midbrain dopamine neurons. Neuron. 2009; 62:826–838. [PubMed: 19555651]

Hasbi A, O'Dowd BF, George SR. Heteromerization of dopamine D2 receptors with dopamine D1 or D5 receptors generates intracellular calcium signaling by different mechanisms. Curr Opin Pharmacol. 2010; 10:93–99. [PubMed: 19897420]

Higley MJ, Sabatini BL. Competitive regulation of synaptic Ca2+ influx by D2 dopamine and A2A adenosine receptors. Nat Neurosci. 2010; 13:958–966. [PubMed: 20601948]

Ikemoto S, Bonci A. Neurocircuitry of drug reward. Neuropharmacology. 2014; 76(Pt B):329–341. [PubMed: 23664810]

Krause M, German PW, Taha SA, Fields HL. A pause in nucleus accumbens neuron firing is required to initiate and maintain feeding. J Neurosci. 2010; 30:4746–4756. [PubMed: 20357125]

Kupchik YM, Brown RM, Heinsbroek JA, Lobo MK, Schwartz DJ, Kalivas PW. Coding the direct/indirect pathways by D1 and D2 receptors is not valid for accumbens projections. Nature neuroscience. 2015; 18:1230–1232. [PubMed: 26214370]

Lim BK, Huang KW, Grueter BA, Rothwell PE, Malenka RC. Anhedonia requires MC4R-mediated synaptic adaptations in nucleus accumbens. Nature. 2012; 487:183–189. [PubMed: 22785313]

Luscher C, Malenka RC. Drug-evoked synaptic plasticity in addiction: from molecular changes to circuit remodeling. Neuron. 2011; 69:650–663. [PubMed: 21338877]

Marcott PF, Mamaligas AA, Ford CP. Phasic dopamine release drives rapid activation of striatal D2-receptors. Neuron. 2014; 84:164–176. [PubMed: 25242218]

McCray JA, Herbette L, Kihara T, Trentham DR. A new approach to time-resolved studies of ATP-requiring biological systems; laser flash photolysis of caged ATP. Proc Natl Acad Sci U S A. 1980; 77:7237–7241. [PubMed: 6938971]

Morikawa H, Khodakhah K, Williams JT. Two intracellular pathways mediate metabotropic glutamate receptor-induced Ca2+ mobilization in dopamine neurons. J Neurosci. 2003; 23:149–157. [PubMed: 12514211]

Nakamura T, Nakamura K, Lasser-Ross N, Barbara JG, Sandler VM, Ross WN. Inositol 1,4,5-trisphosphate (IP3)-mediated Ca2+ release evoked by metabotropic agonists and backpropagating action potentials in hippocampal CA1 pyramidal neurons. J Neurosci. 2000; 20:8365–8376. [PubMed: 11069943]

Partridge JG, Lewin AE, Yasko JR, Vicini S. Contrasting actions of group I metabotropic glutamate receptors in distinct mouse striatal neurones. J Physiol. 2014; 592:2721–2733. [PubMed: 24710062]

Pascoli V, Terrier J, Espallergues J, Valjent E, O'Connor EC, Luscher C. Contrasting forms of cocaine-evoked plasticity control components of relapse. Nature. 2014; 509:459–464. [PubMed: 24848058]

Perreault ML, Hasbi A, O'Dowd BF, George SR. Heteromeric dopamine receptor signaling complexes: emerging neurobiology and disease relevance. Neuropsychopharmacology : official publication of the American College of Neuropsychopharmacology. 2014; 39:156–168. [PubMed: 23774533]

Phillips PE, Stuber GD, Heien ML, Wightman RM, Carelli RM. Subsecond dopamine release promotes cocaine seeking. Nature. 2003; 422:614–618. [PubMed: 12687000]

Plotkin JL, Day M, Surmeier DJ. Synaptically driven state transitions in distal dendrites of striatal spiny neurons. Nat Neurosci. 2011; 14:881–888. [PubMed: 21666674]

Plotkin JL, Shen W, Rafalovich I, Sebel LE, Day M, Chan CS, Surmeier DJ. Regulation of dendritic calcium release in striatal spiny projection neurons. J Neurophysiol. 2013; 110:2325–2336. [PubMed: 23966676]

Power JM, Sah P. Competition between calcium-activated K+ channels determines cholinergic action on firing properties of basolateral amygdala projection neurons. J Neurosci. 2008; 28:3209–3220. [PubMed: 18354024]

Saddoris MP, Sugam JA, Cacciapaglia F, Carelli RM. Rapid dopamine dynamics in the accumbens core and shell: learning and action. Front Biosci (Elite Ed). 2013; 5:273–288. [PubMed: 23276989]

Schiffmann SN, Fisone G, Moresco R, Cunha RA, Ferre S. Adenosine A2A receptors and basal ganglia physiology. Prog Neurobiol. 2007; 83:277–292. [PubMed: 17646043]

Schultz W. Predictive reward signal of dopamine neurons. J Neurophysiol. 1998; 80:1–27. [PubMed: 9658025]

Seidler NW, Jona I, Vegh M, Martonosi A. Cyclopiazonic acid is a specific inhibitor of the Ca2+-ATPase of sarcoplasmic reticulum. J Biol Chem. 1989; 264:17816–17823. [PubMed: 2530215]

Sesack SR, Grace AA. Cortico-Basal Ganglia reward network: microcircuitry. Neuropsychopharmacology. 2010; 35:27–47. [PubMed: 19675534]

Shen W, Flajolet M, Greengard P, Surmeier DJ. Dichotomous dopaminergic control of striatal synaptic plasticity. Science. 2008; 321:848–851. [PubMed: 18687967]

Smith RJ, Lobo MK, Spencer S, Kalivas PW. Cocaine-induced adaptations in D1 and D2 accumbens projection neurons (a dichotomy not necessarily synonymous with direct and indirect pathways). Curr Opin Neurobiol. 2013; 23:546–552. [PubMed: 23428656]

Stern EA, Jaeger D, Wilson CJ. Membrane potential synchrony of simultaneously recorded striatal spiny neurons in vivo. Nature. 1998; 394:475–478. [PubMed: 9697769]

Surmeier DJ, Graves SM, Shen W. Dopaminergic modulation of striatal networks in health and Parkinson's disease. Current opinion in neurobiology. 2014; 29:109–117. [PubMed: 25058111]

Surmeier DJ, Song WJ, Yan Z. Coordinated expression of dopamine receptors in neostriatal medium spiny neurons. The Journal of neuroscience : the official journal of the Society for Neuroscience. 1996; 16:6579–6591. [PubMed: 8815934]

Taha SA, Fields HL. Inhibitions of nucleus accumbens neurons encode a gating signal for reward-directed behavior. J Neurosci. 2006; 26:217–222. [PubMed: 16399690]

Tang TS, Tu H, Wang Z, Bezprozvanny I. Modulation of type 1 inositol (1,4,5)-trisphosphate receptor function by protein kinase a and protein phosphatase 1alpha. J Neurosci. 2003; 23:403–415. [PubMed: 12533600]

Taylor CW, Laude AJ. IP3 receptors and their regulation by calmodulin and cytosolic Ca2+ Cell Calcium. 2002; 32:321–334. [PubMed: 12543092]

Taylor CW, Tovey SC, Rossi AM, Lopez Sanjurjo CI, Prole DL, Rahman T. Structural organization of signalling to and from IP3 receptors. Biochem Soc Trans. 2014; 42:63–70. [PubMed: 24450629]

Tovey SC, Dedos SG, Rahman T, Taylor EJ, Pantazaka E, Taylor CW. Regulation of inositol 1,4,5-trisphosphate receptors by cAMP independent of cAMP-dependent protein kinase. J Biol Chem. 2010; 285:12979–12989. [PubMed: 20189985]

Tritsch NX, Sabatini BL. Dopaminergic modulation of synaptic transmission in cortex and striatum. Neuron. 2012; 76:33–50. [PubMed: 23040805]

Wagner LE 2nd, Joseph SK, Yule DI. Regulation of single inositol 1,4,5-trisphosphate receptor channel activity by protein kinase A phosphorylation. J Physiol. 2008; 586:3577–3596. [PubMed: 18535093]

Walker JW, Feeney J, Trentham DR. Photolabile precursors of inositol phosphates. Preparation and properties of 1-(2-nitrophenyl)ethyl esters of myo-inositol 1,4,5-trisphosphate. Biochemistry. 1989; 28:3272–3280. [PubMed: 2787165]

Wang SS, Denk W, Hausser M. Coincidence detection in single dendritic spines mediated by calcium release. Nat Neurosci. 2000; 3:1266–1273. [PubMed: 11100147]

Wickens JR, Wilson CJ. Regulation of action-potential firing in spiny neurons of the rat neostriatum in vivo. J Neurophysiol. 1998; 79:2358–2364. [PubMed: 9582211]

Wieland S, Schindler S, Huber C, Kohr G, Oswald MJ, Kelsch W. Phasic Dopamine Modifies Sensory-Driven Output of Striatal Neurons through Synaptic Plasticity. J Neurosci. 2015; 35:9946–9956. [PubMed: 26156995]

Wilson CJ, Kawaguchi Y. The origins of two-state spontaneous membrane potential fluctuations of neostriatal spiny neurons. J Neurosci. 1996; 16:2397–2410. [PubMed: 8601819]

Yagishita S, Hayashi-Takagi A, Ellis-Davies GC, Urakubo H, Ishii S, Kasai H. A critical time window for dopamine actions on the structural plasticity of dendritic spines. Science. 2014; 345:1616–1620. [PubMed: 25258080]

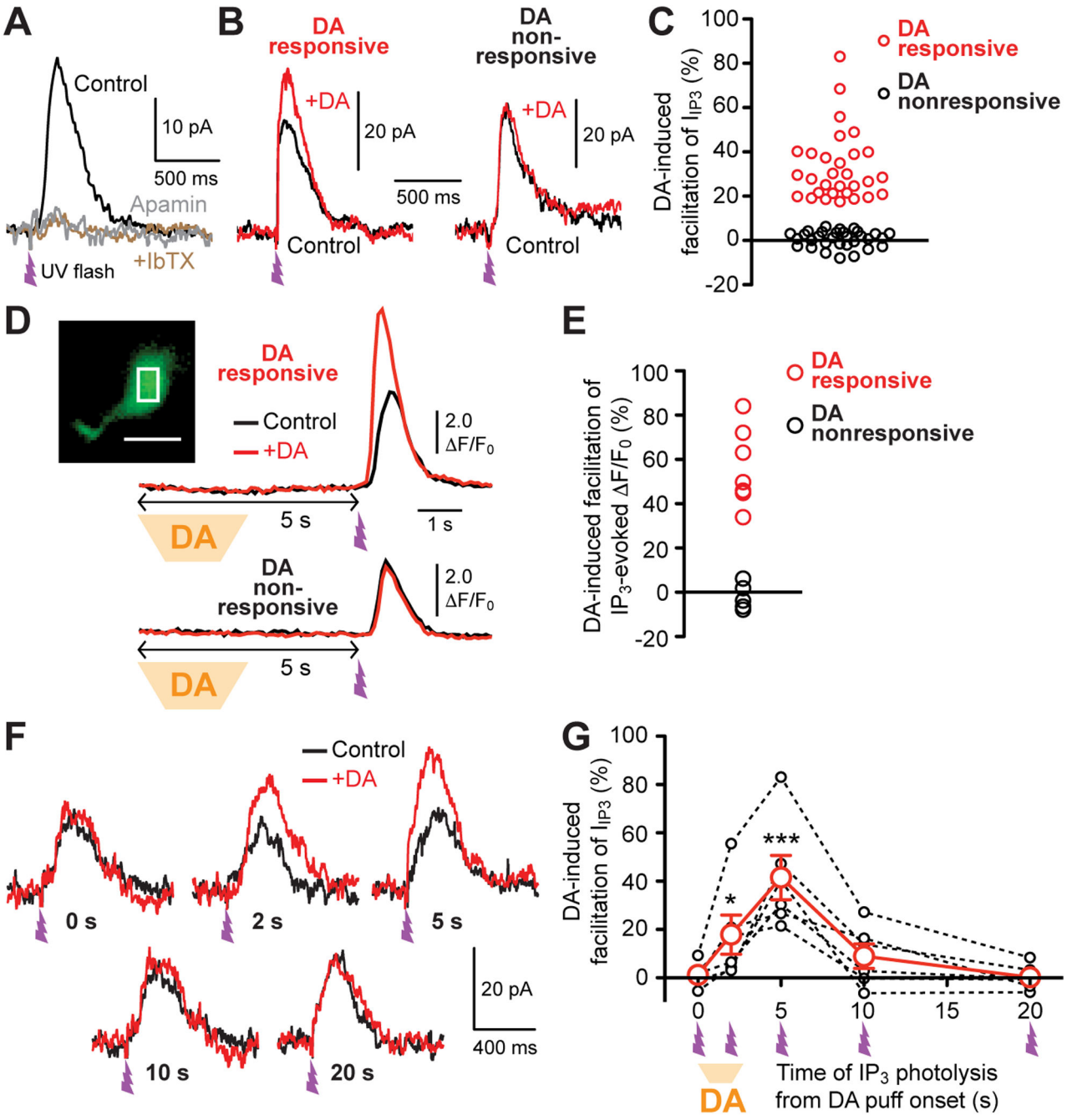

Figure 1. Transient DA application increases IP_3-evoked Ca^{2+} signals in a timingdependent manner in a subpopulation of MSNs

(A) Example traces of I_{IP3} showing that apamin (100 nM) virtually abolished I_{IP3} evoked with submaximal UV flash intensity. UV flash (~1 ms) was applied at the time indicated. Subsequent application of iberiotoxin (IbTX, 100 nM), a selective blocker of large-conductance Ca^{2+}-activated K^+ (BK) channels, had no effect in all 5 cells tested for apamin. (B) Representative I_{IP3} traces with (+DA; red) or without (control; black) preceding DA puff application (2.5 s) in two MSNs. The onset of DA application was 5 s prior to photolytic IP_3

application, as illustrated in (D). Inset (left): Photomicrograph showing the placement of the puff pipette (AC: anterior commissure; scale bar: 200 μm).

(C) Graph plotting the magnitude of I_{IP3} facilitation caused by preceding DA application in individual MSNs (61 cells). Note that a subset of recorded MSNs (30 cells; red) displayed >18% facilitation, whereas no significant DA effect (<5% facilitation) was observed in the remaining MSNs (31 cells; black). See also Figure S1.

(D) Example traces of IP_3-evoked Ca^{2+} transients with (+DA; red) or without (control; black) preceding DA application in two MSNs. Inset: Confocal fluorescence image illustrating the placement of ROI at the soma for fluorescence monitoring (scale bar: 10 μm).

(E) Graph plotting the magnitude of DA-induced facilitation of IP_3-evoked Ca^{2+} transients in individual MSNs (11 cells). DA application produced >30% facilitation of IP_3-evoked Ca^{2+} transients in a subset (6 cells) of these MSNs.

(F) Example traces illustrating the timing dependence of the effects of DA puff application (2.5 s) on I_{IP3}. All traces are from the same MSN. UV flash was applied at the indicated time after the onset of DA application for each red trace.

(G) Summary graph demonstrating the timing dependence of DA-induced I_{IP3} facilitation. Data are from 6 cells that were tested for all 5 intervals shown in (A). *$p < 0.05$, ***$p < 0.001$ vs. data at 0 s (repeated measures one-way ANOVA followed by Bonferroni post hoc test).

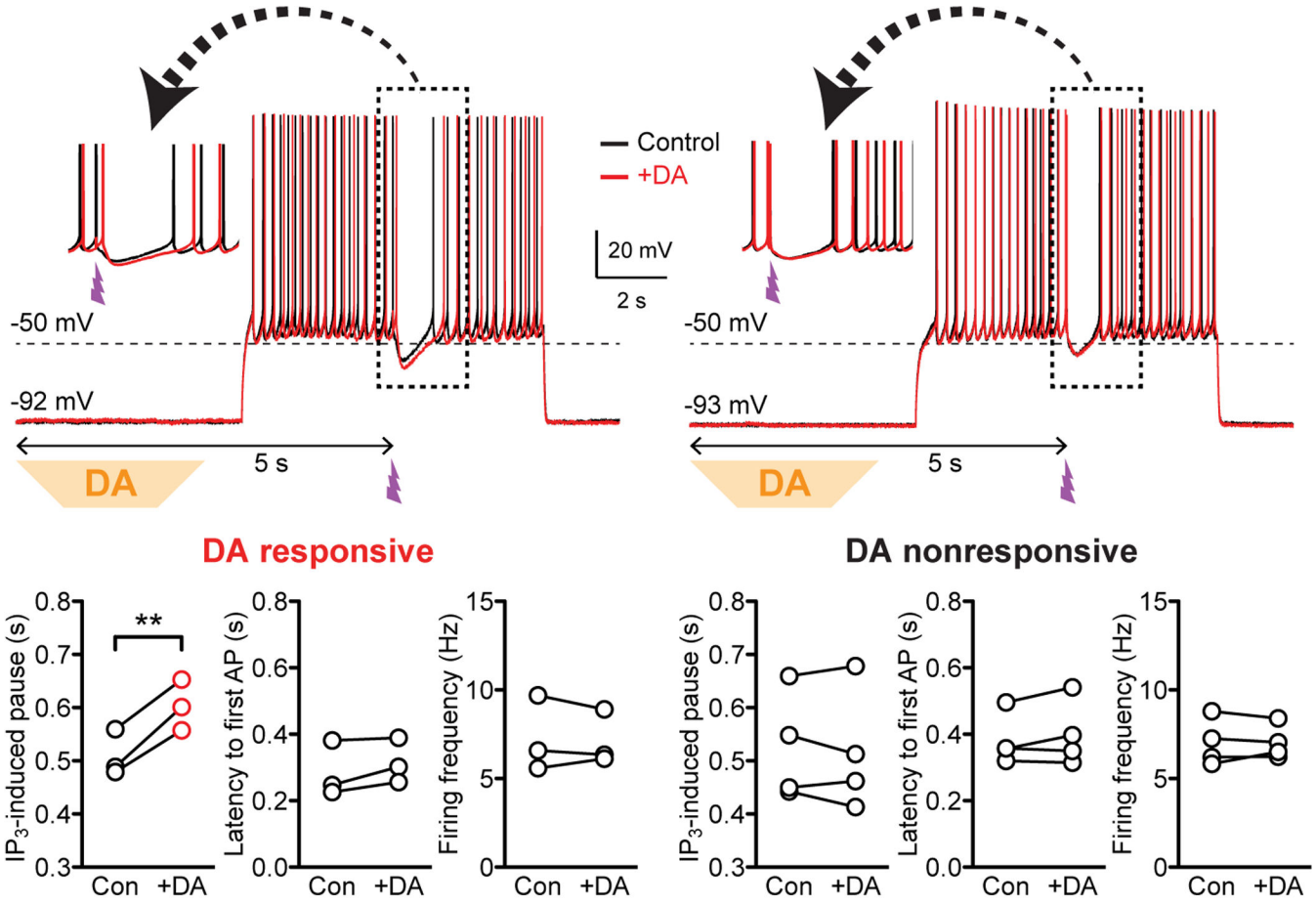

Figure 2. Phasic DA prolongs IP_3-induced pauses in MSN firing

Representative traces (inset: portion in the dashed box shown expanded in timescale) and summary graphs demonstrating the effects of DA puff application on the duration of IP_3-evoked pauses in MSN firing and on firing parameters (latency to the first AP after the onset of depolarizing current injection and the average firing frequency before IP_3 application). DA responsiveness was first determined in voltage clamp (see Figure S2). **$p < 0.01$ (paired t test). See also Figure S2.

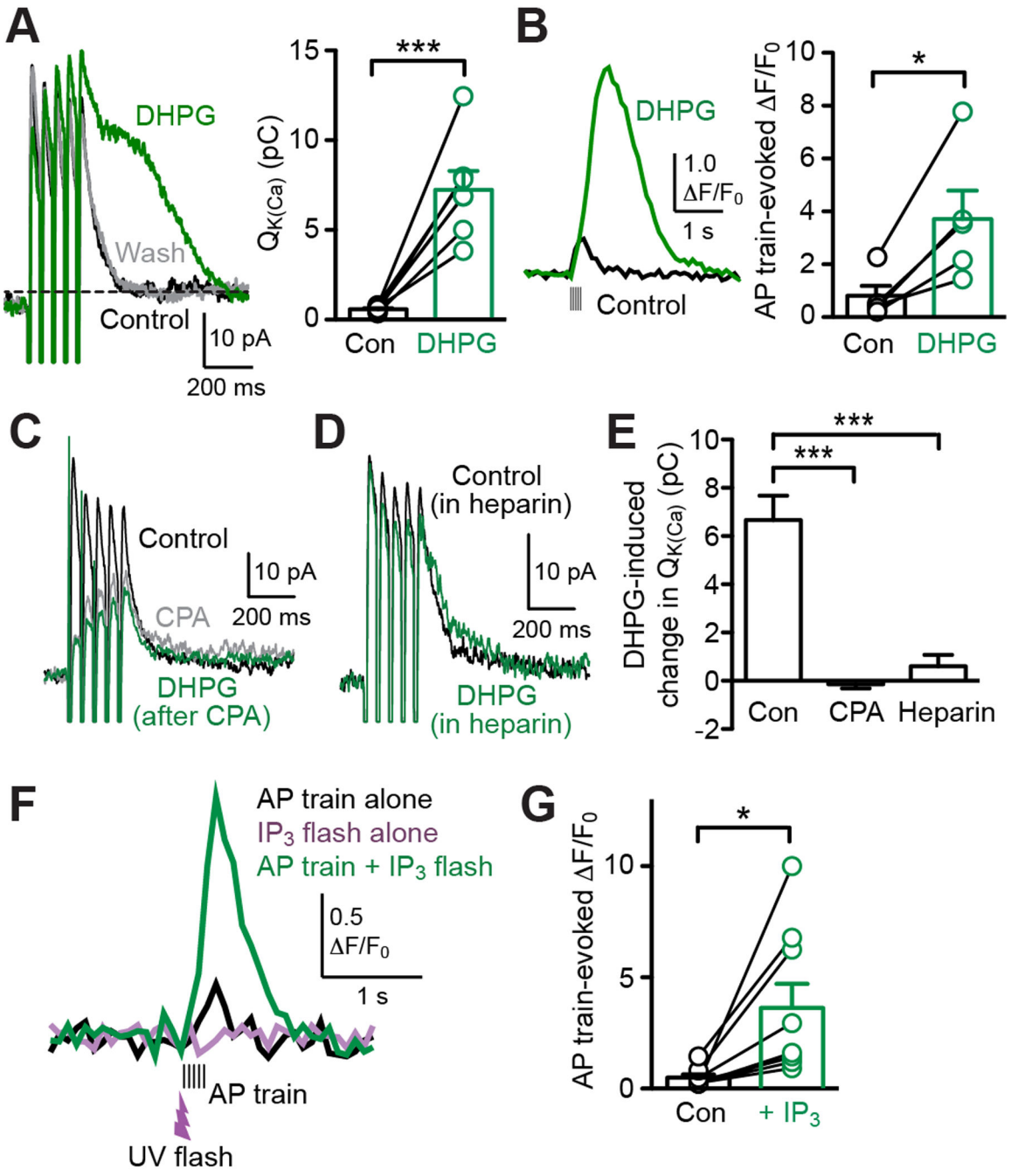

Figure 3. mGluR activation enhances AP train-evoked Ca^{2+} signals via IP_3-dependent CICR from intracellular Ca^{2+} stores

(A) Left: Example traces illustrating the effect of DHPG (5 μM) on $I_{AP\text{-}train}$. Right: Summary graph showing DHPG effect on $Q_{K(Ca)}$ for $I_{AP\text{-}train}$ (7 cells). ***$p < 0.001$ (paired t test). See also Figures S3 and S4.

(B) Example traces (left) and summary graph (right) demonstrating DHPG-induced facilitation of AP train-evoked Ca^{2+} transients monitored with Fluo-4FF (100 μM; 5 cells). *$p < 0.05$ (paired t test).

(C) Representative traces depicting that DHPG had no effect on $I_{AP\text{-}train}$ after depleting intracellular Ca^{2+} stores with CPA (20 μM).
(D) Example traces illustrating small DHPG effect on $I_{AP\text{-}train}$ in a cell loaded with heparin (0.1 mg/ml).
(E) Summary bar graph showing that CPA (n = 5 cells) and heparin (0.1–0.25 mg/ml; n = 5 cells) suppressed DHPG-induced increases in $Q_{K(Ca)}$ observed under control condition (n = 7 cells). ***$p < 0.001$ (one-way ANOVA followed by Bonferroni post hoc test).
(F) Representative traces of Ca^{2+} transients evoked by an AP train alone (black) or by an AP train paired with preceding photolysis of caged IP_3 (green). UV flash (~1 ms) was applied 50 ms prior to the AP train. Note that UV flash intensity was adjusted to evoke no measurable Ca^{2+} rise by itself (purple trace).
(G) Summary graph showing increases in AP train-evoked Ca^{2+} signals by preceding subthreshold IP_3 application (9 cells). *$p < 0.05$ (paired t test). See also Figure S5.

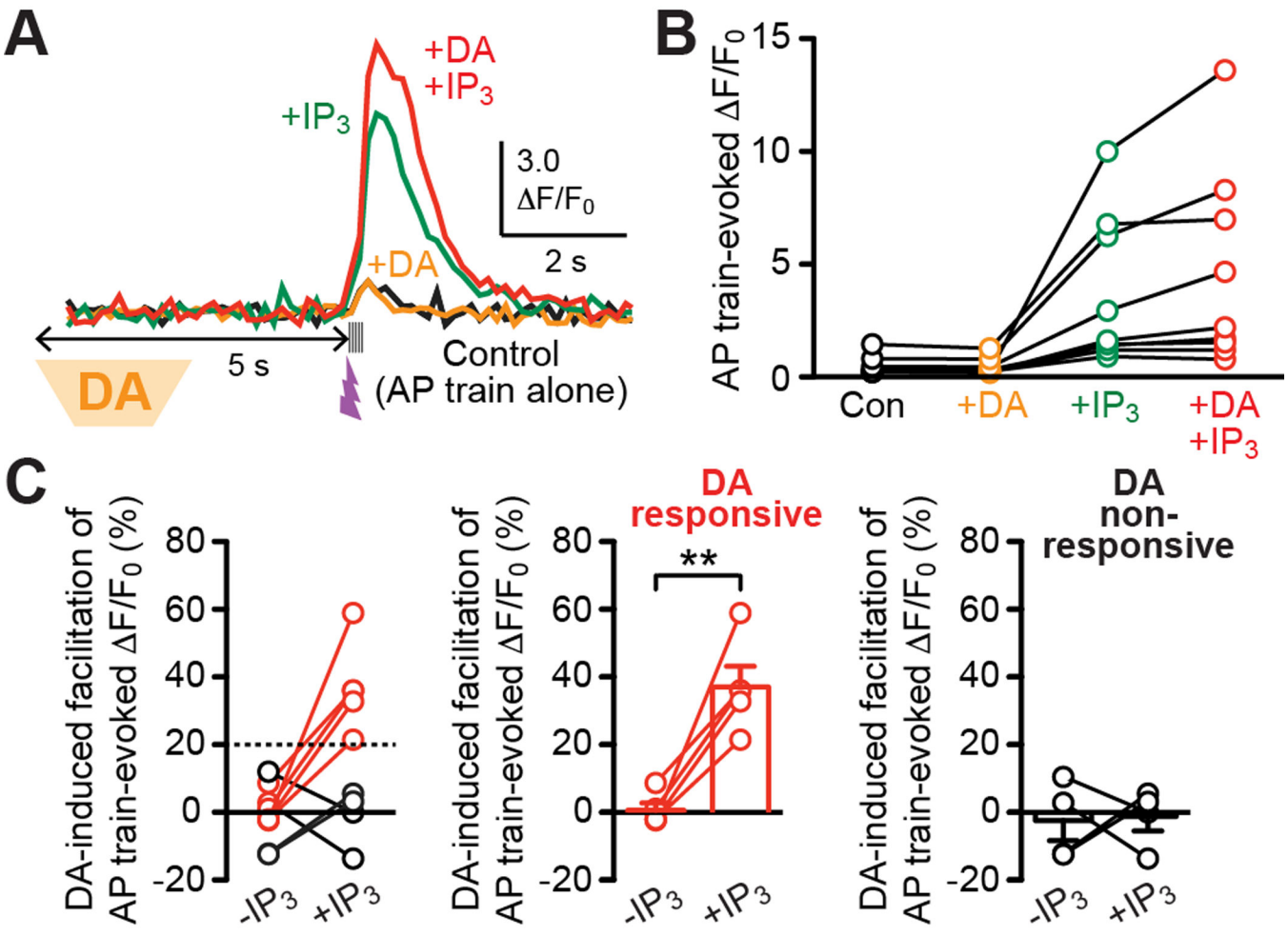

Figure 4. Phasic DA promotes IP_3 facilitation of AP train-evoked Ca^{2+} signals in a subpopulation of MSNs

(A) Example traces of Ca^{2+} transients evoked by an AP train alone (black) or AP trains paired with preceding DA application (orange), with preceding subthreshold IP_3 application (green), or with both DA and IP_3 applications (red). The onset of DA puff application (2.5 s) was set at 5 s prior to the AP train, while UV flash (~1 ms) was applied 50 ms before the AP train.

(B) Graph plotting AP train-evoked Ca^{2+} transients in 9 cells tested for the effects of DA/IP_3 applications as in (A).

(C) Left: The magnitude of phasic DA-induced facilitation of AP train-evoked Ca^{2+} transients are plotted under control condition without IP_3 application [$-IP_3$; facilitation calculated by comparing black and orange traces/data points in (A) and (B)] and with IP_3 application [$+IP_3$; facilitation calculated by comparing green and red traces/data points in (A) and (B)] in all 9 cells shown in (B). Note that DA produced >20% facilitation of AP train-evoked Ca^{2+} transients with IP_3 application in 5 cells (middle), while no measurable DA effect was observed in the remaining 4 cells (right). **$p < 0.01$ (paired t test).

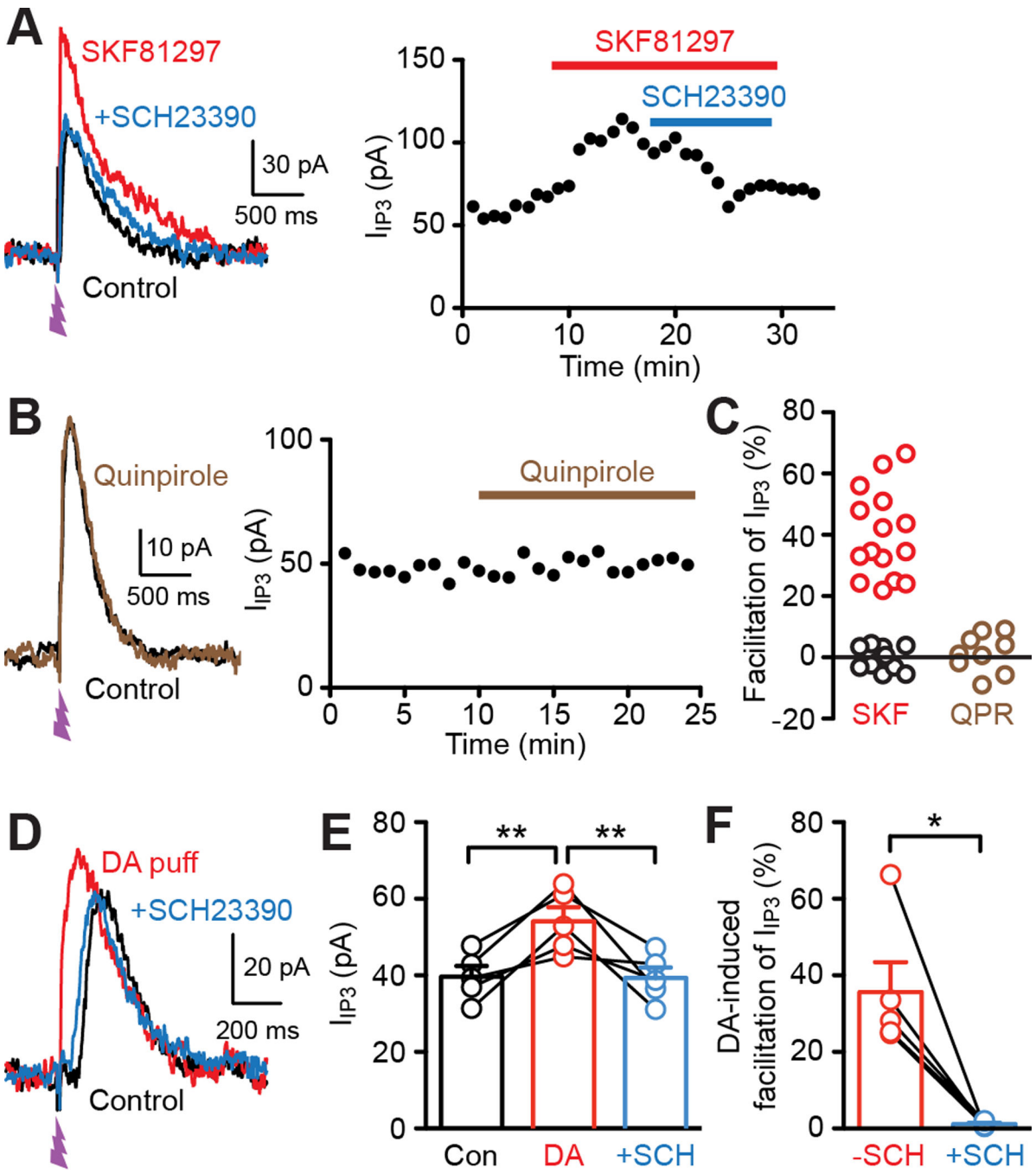

Figure 5. D1 DA receptors mediate facilitation of IP_3-induced Ca^{2+} signals

(A) Example traces (left) and time graph (right) demonstrating the facilitatory effect of the D1 agonist SKF81297 (1 μM) on I_{IP3} and its reversal by the D1 antagonist SCH23390 (1 μM).

(B) Example traces (left) and time graph (right) showing that the D2 agonist quinpirole (1 μM) failed to affect I_{IP3}.

(C) Graph plotting the magnitude of I_{IP3} facilitation produced by SKF81297 (27 cells) or quinpirole (9 cells) in individual MSNs. Data from MSNs showing SKF81297-induced facilitation of I_{IP3} >20% (15 cells) are marked in red.
(D) Representative traces illustrating the blockade of phasic DA-induced facilitation of I_{IP3} by SCH23390.
(E) Summary graph plotting I_{IP3} amplitude in control, with preceding DA application, and with DA application in the presence of SCH23390 (5 cells). **$p < 0.01$ (repeated measures one-way ANOVA followed by Bonferroni post hoc test).
(F) Summary graph plotting the magnitude of DA-induced facilitation of I_{IP3} before (−SCH) and after SCH23390 application (+SCH) in the 5 cells shown in (E). *$p < 0.05$ (paired t test).

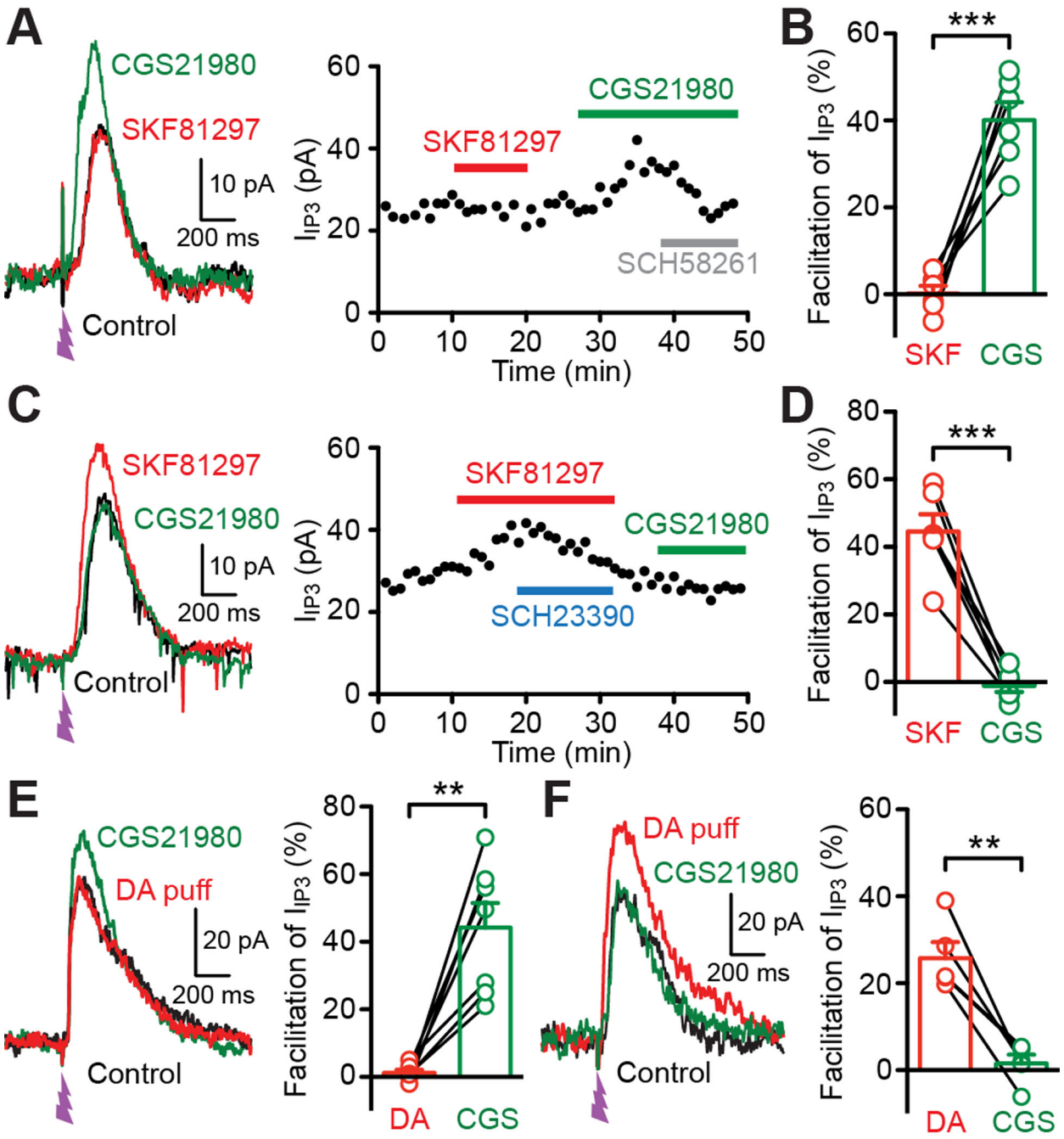

Figure 6. Adenosine A2A receptor activation drives facilitation of IP_3-induced Ca^{2+} signals in MSNs insensitive to D1 DA receptor activation

(A) Representative traces (left) and time graph (right) showing that the A2A agonist CGS21680 (1 μM) augmented I_{IP3} in an MSN that exhibited no response to the D1 antagonist SCH23390 (1 μM). Note in the time graph that the A2A antagonist SCH58261 (1 μM) reversed the effect of CGS21680.

(B) Graph plotting the magnitude of I_{IP3} facilitation in MSNs where I_{IP3} was insensitive to SCH23390 but sensitive to CGS21680 (6 cells).

(C) Example traces (left) and time graph (right) illustrating that CGS21680 failed to affect I_{IP3} in an MSN in which SCH23390 facilitated I_{IP3}.
(D) Graph plotting the magnitude of I_{IP3} facilitation in MSNs where I_{IP3} was sensitive to SCH23390 but insensitive to CGS21680 (6 cells).
(E) Example traces (left) and summary graph (right) showing that CGS21680 facilitated I_{IP3} in MSNs in which DA puff application (2.5 s, onset 5 s before UV flash) failed to affect I_{IP3} (7 cells).
(F) Example traces (left) and summary graph (right) showing that CGS21680 failed to affect I_{IP3} in MSNs where I_{IP3} was enhanced by preceding DA application (5 cells).

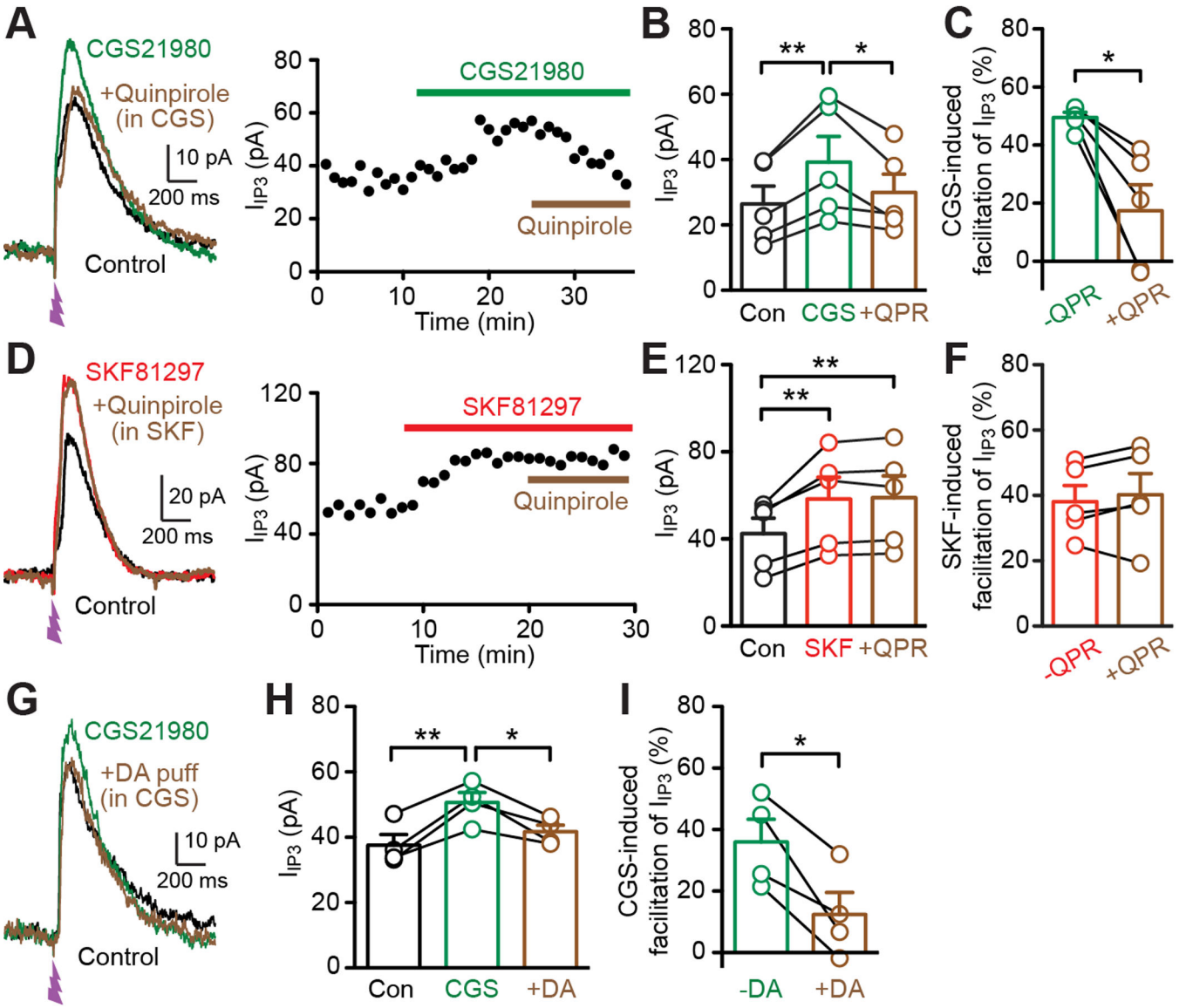

Figure 7. D2 DA receptor activation counteracts adenosine A2A receptor-mediated facilitation of IP_3-induced Ca^{2+} signals

(A) Representative traces (left) and time graph (right) illustrating the reversal of CGS21680 (1 μM)-induced facilitation of I_{IP3} by the D2 agonist quinpirole (1 μM).

(B) Graph plotting I_{IP3} amplitude in control, in CGS21680, and in quinpirole in the continued presence of CGS21680 (5 cells). *p < 0.05, **p < 0.01 (repeated measures one-way ANOVA followed by Bonferroni post hoc test).

(C) Graph plotting the magnitude of CGS21680-induced facilitation of I_{IP3} before (−QPR) and after quinpirole application (+QPR) in the 5 cells shown in (B). *p < 0.05 (paired t test).

(D) Representative traces (left) and time graph (right) depicting the ineffectiveness of quinpirole in reversing SKF81297-induced facilitation of I_{IP3}.

(E) Graph plotting I_{IP3} amplitude in control, in SKF81297, and in quinpirole in the continued presence of SKF81297 (5 cells). **p < 0.01 (repeated measures one-way ANOVA followed by Bonferroni post hoc test).

(F) Graph plotting the magnitude of SKF81297-induced facilitation of I_{IP3} before (−QPR) and after quinpirole application (+QPR) in the 5 cells shown in (E).
(G) Example traces illustrating that DA puff application (2.5 s, onset 5 s prior to UV flash) inhibited I_{IP3} enhanced by CGS21680 perfusion.
(H) Graph plotting I_{IP3} amplitude in control, in CGS21680, and with preceding DA application in the continued presence of CGS21680 (4 cells). *$p < 0.05$, **$p < 0.01$ (repeated measures one-way ANOVA followed by Bonferroni post hoc test).
(I) Graph plotting the magnitude of CGS21680-induced facilitation of I_{IP3} without (−DA) and with DA puff application (+DA) in the 4 cells shown in (H). *$p < 0.05$ (paired t test).